

## Influence of the atomic-scale structure on the exciton fine-structure splitting in InGaAs and GaAs quantum dots in a vertical electric field

Jun-Wei Luo,<sup>1</sup> Ranber Singh,<sup>2</sup> Alex Zunger,<sup>3</sup> and Gabriel Bester<sup>2</sup>

<sup>1</sup>National Renewable Energy Laboratory, Golden, Colorado 80401, USA

<sup>2</sup>Max-Planck-Institut für Festkörperforschung, Heisenbergstrasse 1, D-70569 Stuttgart, Germany

<sup>3</sup>University of Colorado, Boulder, Colorado 80309, USA

(Received 13 July 2012; published 10 October 2012)

We investigate the vertical electric field tuning of the exciton fine-structure splitting (FSS) in several InGaAs and GaAs quantum dots (QDs) using the atomistic empirical pseudopotential approach and configuration interaction. We find that the FSS is surprisingly tunable, with a rate similar to the one reported for lateral electric fields. The minimum FSS for GaAs QDs often lies below the radiative linewidth, which makes them good candidates for the generation of entangled photon pairs. We highlight, however, that random alloy fluctuations affect the minimum FSS by  $\pm 1.4 \mu\text{eV}$ , so that a postselection of QDs may still be beneficial to obtain entangled photon pairs with the highest fidelity. We suggest a simple experimental procedure for this task. The FSS is therefore a rare observable, where the specific decoration of the random alloy lattice matters significantly.

DOI: [10.1103/PhysRevB.86.161302](https://doi.org/10.1103/PhysRevB.86.161302)

PACS number(s): 78.67.Hc, 03.67.Bg, 42.50.Dv, 73.21.La

One of the leading proposals for *on demand* generation of polarization entangled photons is the utilization of the cascade decay of biexciton-exciton-ground state<sup>1</sup> in semiconductor quantum dots (QDs)<sup>2</sup> as illustrated schematically in Fig. 1(a). A serious impediment to the success of this proposal is the existence of a natural splitting within the single exciton manifold [Fig. 1(a)] called “fine-structure splitting” (FSS) that must be suppressed below the radiative linewidth ( $\approx 1 \mu\text{eV}$ ). The FSS is affected by the atomistic symmetry of the QD confining potentials<sup>3–8</sup> and can be manipulated by strain,<sup>9,10</sup> lateral electric fields,<sup>11</sup> vertical electric fields,<sup>12–14</sup> magnetic field,<sup>15</sup> and strong coherent lasers.<sup>16,17</sup> A number of surprising puzzles surround the tuning of the FSS by a vertical electric field. First, it is predicted theoretically,<sup>18</sup> and confirmed experimentally<sup>10,13</sup> and theoretically,<sup>19</sup> that for QDs made of random alloys (with symmetry lower than  $C_{2v}$ ) the two bright components of the excitons undergo an *anticrossing* as a function of fields applied along the  $\{100\}$  or  $\{110\}$  directions.<sup>18</sup> Second, since it has been established that the FSS is related to the atomistic in-plane asymmetry between the  $[110]$  and  $[1\bar{1}0]$  crystallographic directions, it would appear that such an intrinsic quantity would not lend itself to tuning via a *vertical* field. Nevertheless, it was shown experimentally that the FSS can be tuned rather effectively in In(Ga)As/GaAs QDs by applying an electric field along the growth direction.<sup>13</sup> Third, the role of strain is unclear: While electric field control was observed in strain-free monolayer thickness fluctuation GaAs QDs,<sup>12,14</sup> investigations of this effect for other strain-free GaAs QDs grown by multistep hierarchical self-assembly<sup>20</sup> or droplet epitaxy<sup>21</sup> are needed. Finally, even though strain-free GaAs/AlGaAs QDs naturally lack the built-in strain asymmetry that was believed to contribute to FSS in strained InAs/GaAs QDs,<sup>22</sup> significant FSS can still exist, casting doubt on our understanding of the role of strain in creating FSS-promoting asymmetries in the potential.

Here, we clarify the physical process underlying the tuning of the FSS by vertical electric fields by developing a simple mesoscopic model that allows us to analyze our million atom calculations of a large set of InGaAs/GaAs and GaAs/AlGaAs

QDs. We find good agreement of our results for InGaAs QDs with existing experiments<sup>13</sup> and predict that the FSS in strain-free GaAs/AlGaAs QDs is tunable well below the radiative linewidth ( $\approx 1 \mu\text{eV}$ ). However, we show that different decorations of the cation lattice in the AlGaAs alloy barrier lead to fluctuations in the minimum FSS in the range of  $\pm 1.4 \mu\text{eV}$ , making a postselection of appropriate QDs necessary. We show that measurements of the FSS and the polarization angle at zero field suffice to identify appropriate QDs.

We consider lens-shaped and Gaussian-shaped QDs with sizes, composition, and material as given in Table I. The atom positions are relaxed using the valence force field method.<sup>23</sup> The single particle states are calculated using the atomistic empirical pseudopotential approach,<sup>23,24</sup> taking strain, band coupling, coupling between different parts of the Brillouin zone, and spin-orbit coupling into account, for multi-million atom structures. We apply an external electric field following Ref. 25. The direct and exchange Coulomb interactions are calculated from the atomic wave functions as shown in Ref. 6, and the correlated excitonic states are calculated by the configuration interaction (CI) approach<sup>26</sup> using 12 electron and 12 hole states (spin included), thus accounting for correlations.

Before we present our numerical results, we introduce a mesoscopic simple model where the Hamiltonian is split into different components:

$$H = H_{C_{2v}} + \delta H_{C_1} + q_s Fz, \quad (1)$$

where  $q_s$  is the charge of a particle in band  $s$ , i.e.,  $-e$  ( $+e$ ) for conduction (valence) bands,  $H_{C_{2v}}$  is the Hamiltonian of the QD with  $C_{2v}$  point group symmetry, which must be supplemented by the deviation from this symmetry by the term  $\delta H_{C_1}$ . This latter term represents the random alloy present in the barrier and possible impurities inside the GaAs QD, as well as shape asymmetries. In the space of the two bright states  $|1\rangle$  and  $|2\rangle$  the Hamiltonian has a simple form:

$$H = \begin{pmatrix} E_1 + \delta E_1 + \gamma_1 F & s_0/2 \\ s_0/2 & E_2 + \delta E_2 + \gamma_2 F \end{pmatrix}. \quad (2)$$

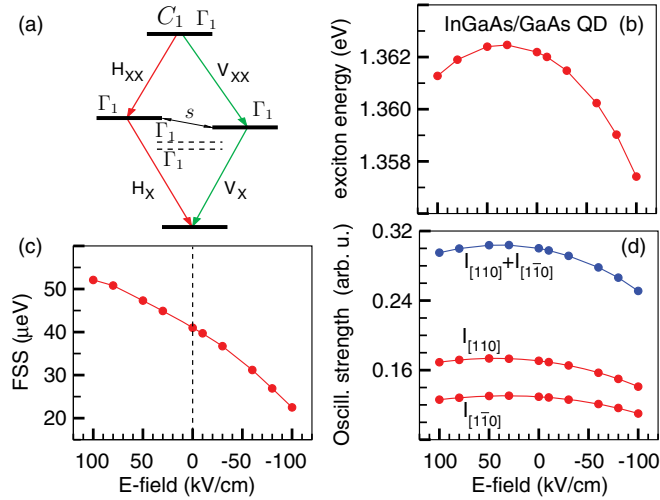


FIG. 1. (Color online) (a) Schematic representation of the biexciton  $\rightarrow$  exciton  $\rightarrow$  ground – state cascade. (b) Exciton energy, (c) FSS, and (d) oscillator strength of the bright exciton transitions along the  $[110]$  and  $[1\bar{1}0]$  directions as a function of applied electric field for the strained InGaAs/GaAs QD00 (see Table I).

The exciton energies of the high symmetric hypothetical structure given by  $E_1 = \langle 1|H_{C_{2v}}|1\rangle$  and  $E_2 = \langle 2|H_{C_{2v}}|2\rangle$  are different due mainly to strain<sup>22</sup> (nearly vanishing in the case of strain-free GaAs QDs). The lowering of the symmetry to  $C_1$  leads to the terms  $\delta E_1 = \langle 1|\delta H_{C_1}|1\rangle$  and  $\delta E_2 = \langle 2|\delta H_{C_1}|2\rangle$  and also to  $s_0/2 = \langle 1|\delta H_{C_1}|2\rangle$  and  $\gamma_i = \langle i|q_s z|i\rangle$ . Redefining  $E_1 + \delta E_1$  as  $E_0$  and  $\delta = E_2 - E_1 + \delta E_2 - \delta E_1$  and removing the linear term in the field from  $|1\rangle$  leads to

$$H = \begin{pmatrix} E_0 & s_0/2 \\ s_0/2 & E_0 + \delta + (\gamma_2 - \gamma_1)F \end{pmatrix}, \quad (3)$$

TABLE I. Sizes and compositions of different QDs investigated in this paper. The sizes  $a$ ,  $b$ , and  $h$  describe the elliptic axis along the  $[110]$  and  $[1\bar{1}0]$  directions and the height, respectively.

| QD             | Composition                              | Size (nm)<br>$a, b, h$ | Barrier (% Al) |        |
|----------------|--|------------------------|----------------|--------|
|                |  |                        | Top            | Bottom |
| Lens shape     |  |                        |                |        |
| 00             | In <sub>0.8</sub> Ga <sub>0.2</sub> As   | 10, 7.5, 2.5           | 0              | 0      |
| 01             | GaAs                                     | 45, 45, 3              | 35             | 35     |
| 02             | GaAs                                     | 70, 50, 3              | 45             | 45     |
| 03             | GaAs                                     | 70, 50, 3              | 35             | 45     |
| 04             | GaAs                                     | 60, 40, 2              | 35             | 45     |
| 05             | GaAs                                     | 25, 31, 3.9            | 35             | 35     |
| Gaussian shape |  |                        |                |        |
| 06             | GaAs                                     | 30, 30, 3              | 30             | 30     |
| 07             | GaAs                                     | 30, 30, 4              | 30             | 30     |
| 08             | GaAs                                     | 30, 30, 6              | 30             | 30     |
| 09             | GaAs                                     | 35, 30, 3              | 30             | 30     |
| 10             | GaAs                                     | 35, 30, 4              | 30             | 30     |
| 11             | GaAs                                     | 35, 30, 6              | 30             | 30     |
| 12             | Al <sub>0.06</sub> Ga <sub>0.94</sub> As | 30, 30, 3              | 30             | 30     |
| 13             | Al <sub>0.06</sub> Ga <sub>0.94</sub> As | 30, 30, 6              | 30             | 30     |
| 14             | Al <sub>0.06</sub> Ga <sub>0.94</sub> As | 35, 30, 3              | 30             | 30     |
| 15             | Al <sub>0.06</sub> Ga <sub>0.94</sub> As | 35, 30, 6              | 30             | 30     |

which corresponds to the anticrossing model used by Bennett *et al.*<sup>13</sup>

$$E \begin{pmatrix} \cos \theta \\ \sin \theta \end{pmatrix} = \begin{pmatrix} E_0 & s_0/2 \\ s_0/2 & E_0 - \gamma(F - F_0) \end{pmatrix} \begin{pmatrix} \cos \theta \\ \sin \theta \end{pmatrix}. \quad (4)$$

We identify  $\gamma = \gamma_1 - \gamma_2$  and  $\gamma F_0 = \delta$  from Eqs. (2) and (4). This simple reformulation clarifies the origin of the terms,  $\gamma$  being the difference in the response of  $|1\rangle$  and  $|2\rangle$  to the applied field and  $\gamma F_0$  being the intrinsic FSS due to the inequivalence of  $[110]$  and  $[1\bar{1}0]$  in  $C_{2v}$  (small for a strain free structure) and the lowering to  $C_1$  symmetry through atomistic alloy effects.  $s_0$  is the FSS at the anticrossing and quantifies the coupling between the bright states. In a pure GaAs QD embedded in a pure AlAs matrix the bright states are expected to cross<sup>18</sup> due to the high  $C_{2v}$  symmetry of the structure and  $s_0 = 0$ . However, the reduction of the QD symmetry due to the alloy fluctuations in the AlGaAs barrier at the QD interface leads to an avoided crossing<sup>18</sup> with  $s_0/2 \neq 0$ .  $F_0$  is the field at the anticrossing. As the field approaches  $F_0$ , the exciton eigenstates become a coherent mixture with components  $\sin \theta$  and  $\cos \theta$ , where  $\theta$  is the angle describing the orientation of the lowest eigenstate relative to the  $[110]$  crystal axis. The solution of Eq. (4) yields the eigenvalues ( $E_{\pm}$ ) and angles:<sup>13</sup>

$$E_{\pm} = E_0 - \frac{\gamma(F - F_0)}{2} \pm \frac{1}{2} \sqrt{\gamma^2(F - F_0)^2 + s_0^2}, \quad (5)$$

$$\theta = \pm \tan^{-1} \left[ \frac{s_0}{\gamma(F - F_0) \pm (E_- - E_+)} \right]. \quad (6)$$

We note at this point that the model of Eq. (2) does not include any field dependence of the off-diagonal terms. Such terms would lead to an additional coupling of the two bright states and could be used to tune the FSS through zero (if it would exactly compensate  $s_0/2$ ). In our case of vertical field, this coupling is negligible, but in the case of a field with a component along a low symmetry direction (any direction but  $[110]$  or  $[1\bar{1}0]$ ) this term should exist. A future investigation of this effect would be worthwhile.

We first present our results for the strained In<sub>0.8</sub>Ga<sub>0.2</sub>As QD00 (see Table I), an emission energy that fits the measured results of Bennett *et al.*<sup>13</sup> very well. Figure 1 shows the Stark shift, FSS, and the oscillator strength as a function of vertical electric field. We obtain a nearly linear change in the FSS with the  $E$  field in agreement with the experimental results.<sup>13</sup> A fit of our numerical results to the model of Eq. (4) yields the parameters given in Table II. For the field dependence of the FSS,  $\gamma$ , we obtain a value of  $0.15 \mu\text{eV cm/kV}$ , somewhat lower than the value of  $0.28 \mu\text{eV cm/kV}$  reported by Bennett *et al.*<sup>13</sup> The strong shape and size dependence of the slope can explain this discrepancy and will be illustrated below. Our results for the set of strain-free GaAs QDs given in Table I are shown in Figs. 2 and 3, where we plotted the Stark shift, the FSSs, the polarization angle  $\theta$ , and the oscillator strength as a function of the vertical  $E$  field. The results of the fit to the model of Eq. (4) are given in Table II. We make the following observations.

*FSS and polarization angle.* The anticrossing described by Eq. (4) can be seen in Figs. 2(c) and 3 as a reduction of the FSS until the value  $s_0$ , followed by an increase. The anticrossing is accompanied by a rotation of the polarization angle of the

TABLE II. Transition energy  $E_0$  and FSS parameters defined in Eq. (4) and extracted from our numerical results. The error bars represent the range of parameters we obtain by running five different random alloy realizations (see Fig. 3).

| QD | $E_0$<br>(meV) | $s_0$<br>( $\mu\text{eV}$ ) | $\gamma$<br>( $\mu\text{eV cm/kV}$ ) | $F_0$<br>(kV/cm) |
|----|----------------|-----------------------------|--------------------------------------|------------------|
| 00 | 1363           | ?                           | 0.15                                 | + 273            |
| 01 | 1644           | 0.1                         | 0.11                                 | + 17             |
| 02 | 1650           | 0.1                         | 0.08                                 | - 48             |
| 03 | 1643           | 0.1                         | 0.08                                 | - 48             |
| 04 | 1742           | 0.9                         | 0.14                                 | - 43             |
| 05 | 1679           | 0.3                         | 0.33                                 | + 29             |
| 06 | $1762 \pm 2$   | $0.8 \pm 0.3$               | $0.85 \pm 0.08$                      | $-21 \pm 5$      |
| 07 | $1718 \pm 2$   | $0.4 \pm 0.1$               | $0.95 \pm 0.06$                      | $-26 \pm 3$      |
| 08 | $1666 \pm 1$   | $0.9 \pm 0.8$               | $1.06 \pm 0.07$                      | $-25 \pm 2$      |
| 09 | 1754           | 0.9                         | 0.79                                 | -33.5            |
| 10 | 1714           | 0.4                         | 0.78                                 | -37.4            |
| 11 | 1660           | 0.7                         | 0.96                                 | -40.5            |
| 12 | $1806 \pm 5$   | $1.2 \pm 0.7$               | $0.74 \pm 0.11$                      | $-14 \pm 7$      |
| 13 | $1727 \pm 2$   | $1.2 \pm 0.5$               | $0.85 \pm 0.09$                      | $-15 \pm 9$      |
| 14 | $1799 \pm 2$   | $1.3 \pm 1.0$               | $0.73 \pm 0.03$                      | $-25 \pm 6$      |
| 15 | $1721 \pm 2$   | $1.8 \pm 1.4$               | $0.84 \pm 0.07$                      | $-40 \pm 5$      |

lowest energy exciton state,<sup>18</sup> as shown in Fig. 2(a). At the field  $F_0$ , where the anticrossing occurs, the polarization angle changes more rapidly when  $s_0$  is small, in agreement with the model.

*Shape and size effects on the tunability  $\gamma$ .* Table II reveals that  $\gamma$  increases with the height of the QDs: Tall dots are more tunable in the vertical electric field, which are correlated with the polarizability of the exciton states. Comparing QD05 and QD07 with similar dimensions but different shapes shows that Gaussian-shaped dots have a larger  $\gamma$  value.

*Shape and size effects on  $s_0$ .* From Table II we conclude that the shape effect on  $s_0$  is rather moderate, while the size effect shows a trend for larger values of  $s_0$  in larger QDs. This latter trend is, however, overshadowed by a very strong random alloy effect (see next).

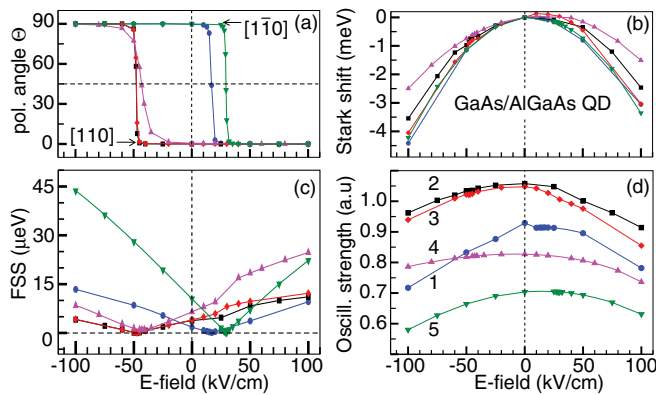


FIG. 2. (Color online) Results for GaAs/AlGaAs strain-free QDs. (a) Polarization angle  $\theta$ , (b) Stark shift, (c) FSS, and (d) sum of intensities along the [110] and the  $[1\bar{1}0]$  crystal directions as a function of applied vertical  $E$  field. The circles, squares, diamonds, uptriangles, and downtriangles are for the QD01, QD02, QD03, QD04, and QD05, respectively.

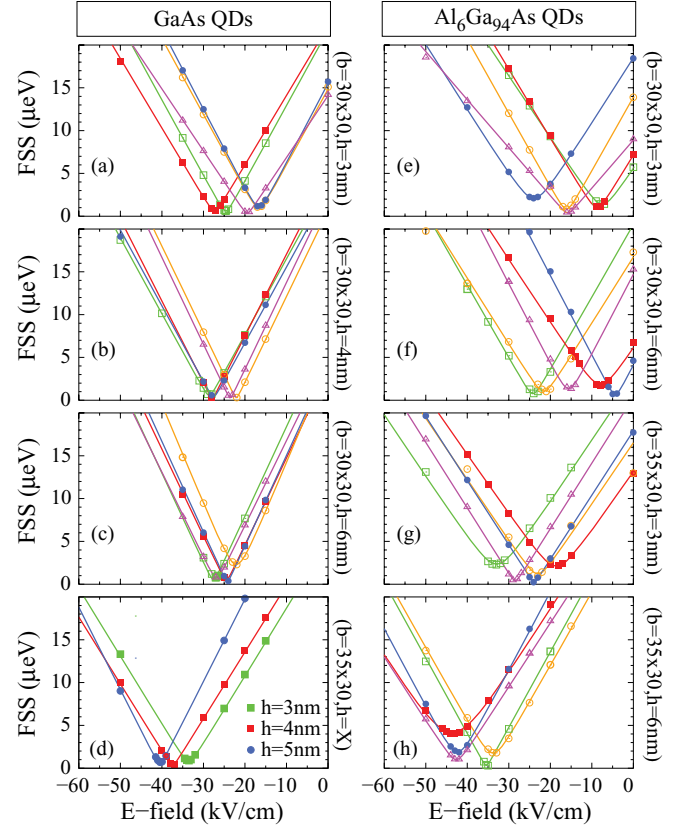


FIG. 3. (Color online) FSS as a function of the electric field for various QDs listed in Table I. Five different alloy configurations of the  $\text{Al}_{30}\text{Ga}_{70}\text{As}$  matrix have been used in (a)–(c), and five different QD alloy configurations in (e)–(h).

*Random alloy effects on  $s_0$  and  $F_0$ .* In Figs. 3(a)–3(c) we generated the same QD structure with different random realizations of the barrier material. In Figs. 3(e)–3(g) the QDs have a 6% Al content and these Al atoms are randomly distributed in five different realizations within the QDs. These variations represent fluctuations that should be encountered experimentally. We notice that both  $s_0$  and  $F_0$  are significantly affected by these atomistic effects. For instance, the pure GaAs QD QD08 can exist with  $s_0$  of 0.1 or 1.7  $\mu\text{eV}$  by merely changing the realization (i.e., the random distribution of the cations) of the barrier material. Furthermore, QD15 can exist with  $s_0$  of 0.4 or 3.2  $\mu\text{eV}$  by changing the random distribution of the 6% Al atoms inside the QD. The sensitivity of  $s_0$  and  $F_0$  on the alloy realization is in agreement with our model [Eq. (2)], where these terms have been shown to originate from the lowering of the symmetry (term  $\delta H_{C_1}$ ).

*Random alloy effect on  $\gamma$ .* The value of  $\gamma$  is only weakly dependent on the details of the alloy realization (see Fig. 3) but rather strongly on the QDs' geometry, size, and composition [see Fig. 2(c)]. Indeed, following our model,  $\gamma$  gives the difference in the response of |1) and |2) to the applied field and is directly related to the light-hole component of the exciton state. For a pure heavy-hole exciton,  $\gamma$  vanishes. The light-hole component does change significantly for different shapes (QD01, QD02, QD03, QD04, QD05 have 3.5%, 2.4%, 2.6%, 5.0%, and 8.2% light-hole components, respectively) but remains constant for different alloy realizations.

*Oscillator strength.* Figure 2(d) shows a moderate change of the oscillator strength, in the range of 10%, with varying  $E$  field in the range of  $-100$  to  $+100$  kV/cm.

*How to select QDs with small  $s_0$ .* Our present work shows that GaAs QDs are good candidates to achieve small FSS via vertical electric field, but also that rather large fluctuations of  $s_0$  should be expected within one homogenous set of QDs (that differ only by random alloy effects and have the same shape, size, and composition). A selection of appropriate QDs (as practiced experimentally<sup>27,28</sup>) will therefore be advantageous, if not necessary. From Eqs. (5) and (6) at zero field ( $F = 0$ ) we can derive the following expressions:

$$F_0 = \frac{\Delta E \cos 2\theta}{\gamma}, \quad s_0 = -\Delta E \sin 2\theta, \quad (7)$$

where  $\Delta E$  is the FSS at  $F = 0$ . Interestingly,  $s_0$  does not depend on the slope  $\gamma$  and only requires a single measurement of the FSS and the corresponding polarization angle  $\theta$  at zero field. We have used Eq. (7) in Table II to report our value of  $F_0$  for QD00. For the value of  $s_0$ , however, if  $\Delta E$  is large, a small inaccuracy in the measurement, or the calculation in our case, of the angle  $\theta$  will lead to an inaccurate determination of  $s_0$ . With a  $\Delta E$  of  $50 \mu\text{eV}$  and an angle accuracy of  $2^\circ$  we obtain  $s_0$  with an error bar of  $\pm 3.5 \mu\text{eV}$ , which is too large to be useful. However, Eq. (7) is very useful for QDs where  $\Delta E$  is not too large, which represent the QDs that will require weaker  $E$  fields to be tuned.

In summary, we showed that the FSS in GaAs/AlGaAs and InGaAs/GaAs self-assembled QDs can be effectively tuned by a vertical electric field. Indeed, the tuning rate for GaAs QDs is between  $0.1$  and  $1 \mu\text{eV cm/kV}$ , depending on

size and geometry, and is surprisingly similar to the tuning rate obtained with lateral electric fields [ $0.15 \mu\text{eV cm/kV}$  (Ref. 29)]. Our results for InGaAs QDs are in good agreement with experiment, while the results for GaAs QDs represent predictions. The minimum FSS,  $s_0$ , for GaAs QDs, is between  $0.1$  and  $1.8 \mu\text{eV}$ , depending on size and geometry. However, alloy fluctuations in the surrounding barrier lead to variations of  $s_0$  in the range of  $\pm 1.4 \mu\text{eV}$ , calling for a postselection of the “best QDs,” for which we suggest a simple experimental procedure requiring only one measurement at zero field.

This dependence of  $s_0$ , and also  $F_0$ , on the random atomic arrangement is in agreement with the expectations from a simple mesoscopic model that shows these terms to be proportional to the “amount of deviation from  $C_{2v}$ ” symmetry towards the lower  $C_1$  symmetry. Hence, a QD made of a random alloy (with formally  $C_1$  symmetry) with an atomic decoration of the lattice that will resemble the  $C_{2v}$  symmetry will have the smallest  $s_0$ . This represents a striking example of an observable, where the conventional treatment of a random alloy through a replacement of the atomic distribution by an average [virtual crystal approximation (VCA)<sup>30</sup>] or an effective medium [coherent-potential approximation (CPA)<sup>30</sup>] fails. In this case, the position of each and every atom in a structure made of several thousand atoms is relevant.

G.B. and R.S. would like to acknowledge financial support by the BMBF (QuaHL-Rep, Contract No. 01BQ1034). The work done by J.W.L. and A.Z. was funded by the US Department of Energy, Office of Science, Basic Energy Science, Materials Sciences and Engineering, under Contract No. DE-AC36-08GO28308 to NREL.

- 
- <sup>1</sup>O. Benson, C. Santori, M. Pelton, and Y. Yamamoto, *Phys. Rev. Lett.* **84**, 2513 (2000).
- <sup>2</sup>*Single Semiconductor Quantum Dots Series: NanoScience and Technology*, edited by P. Michler (Springer, Berlin, 2009).
- <sup>3</sup>M. Bayer, A. Kuther, A. Forchel, A. Gorbunov, V. B. Timofeev, F. Schäfer, J. P. Reithmaier, T. L. Reinecke, and S. N. Walck, *Phys. Rev. Lett.* **82**, 1748 (1999).
- <sup>4</sup>R. J. Warburton, C. Schaflein, D. Haft, F. Bickel, A. Lorke, K. Karrai, J. M. Garcia, and P. M. Petroff, *Nature (London)* **405**, 926 (2000).
- <sup>5</sup>T. Takagahara, *Phys. Rev. B* **62**, 16840 (2000).
- <sup>6</sup>G. Bester, S. Nair, and A. Zunger, *Phys. Rev. B* **67**, 161306(R) (2003).
- <sup>7</sup>L. Besombes, K. Kheng, and D. Martrou, *Phys. Rev. Lett.* **85**, 425 (2000).
- <sup>8</sup>R. Seguin, A. Schliwa, S. Rodt, K. Potschke, U. W. Pohl, and D. Bimberg, *Phys. Rev. Lett.* **95**, 257402 (2005).
- <sup>9</sup>S. Seidl, M. Kroner, A. Hoge, K. Karrai, R. Warburton, A. Badolato, and P. Petroff, *Appl. Phys. Lett.* **88**, 203113 (2006).
- <sup>10</sup>J. Plumhof, V. Křápek, F. Ding, K. Jöns, R. Hafenbrak, P. Klenovský, A. Herklotz, K. Dörr, P. Michler, A. Rastelli *et al.*, *Phys. Rev. B* **83**, 121302 (2011).
- <sup>11</sup>K. Kowalik, O. Krebs, A. Lemaitre, S. Laurent, P. Senellart, P. Voisin, and J. A. Gaj, *Appl. Phys. Lett.* **86**, 041907 (2005).
- <sup>12</sup>S. Marcet, K. Ohtani, and H. Ohno, *Appl. Phys. Lett.* **96**, 101117 (2010).
- <sup>13</sup>A. J. Bennett, M. A. Pooley, R. M. Stevenson, M. B. Ward, R. B. Patel, A. B. d. I. Giroday, N. Sköld, I. Farrer, C. A. Nicoll, D. A. Ritchie *et al.*, *Nat. Phys.* **6**, 947 (2010).
- <sup>14</sup>M. Ghali, K. Ohtani, Y. Ohno, and H. Ohno, *Nat. Commun.* **3**, 661 (2012).
- <sup>15</sup>R. Stevenson, R. Young, P. Atkinson, K. Cooper, D. Ritchie, and A. Shields, *Nature (London)* **439**, 179 (2006).
- <sup>16</sup>G. Jundt, L. Robledo, A. Hoge, S. Fält, and A. Imamoglu, *Phys. Rev. Lett.* **100**, 177401 (2008).
- <sup>17</sup>A. Muller, W. Fang, J. Lawall, and G. S. Solomon, *Phys. Rev. Lett.* **103**, 217402 (2009).
- <sup>18</sup>R. Singh and G. Bester, *Phys. Rev. Lett.* **104**, 196803 (2010).
- <sup>19</sup>M. Gong, W. Zhang, G.-C. Guo, and L. He, *Phys. Rev. Lett.* **106**, 227401 (2011).
- <sup>20</sup>A. Rastelli, S. Stufler, A. Schliwa, R. Songmuang, C. Manzano, G. Costantini, K. Kern, A. Zrenner, D. Bimberg, and O. G. Schmidt, *Phys. Rev. Lett.* **92**, 166104 (2004).
- <sup>21</sup>K. Watanabe, N. Koguchi, and Y. Gotoh, *Jpn. J. Appl. Phys.* **39**, L79 (2000).
- <sup>22</sup>G. Bester and A. Zunger, *Phys. Rev. B* **71**, 045318 (2005).
- <sup>23</sup>A. J. Williamson, L.-W. Wang, and A. Zunger, *Phys. Rev. B* **62**, 12963 (2000).

- <sup>24</sup>L.-W. Wang and A. Zunger, *Phys. Rev. B* **59**, 15806 (1999).
- <sup>25</sup>G. Bester and A. Zunger, *Phys. Rev. B* **72**, 165334 (2005).
- <sup>26</sup>A. Franceschetti, H. Fu, L.-W. Wang, and A. Zunger, *Phys. Rev. B* **60**, 1819 (1999).
- <sup>27</sup>R. J. Young, R. M. Stevenson, A. J. Shields, P. Atkinson, K. Cooper, D. A. Ritchie, K. M. Groom, A. I. Tartakovskii, and M. S. Skolnick, *Phys. Rev. B* **72**, 113305 (2005).
- <sup>28</sup>R. M. Stevenson, C. L. Salter, J. Nilsson, A. J. Bennett, M. B. Ward, I. Farrer, D. A. Ritchie, and A. J. Shields, *Phys. Rev. Lett.* **108**, 040503 (2012).
- <sup>29</sup>M. M. Vogel, S. M. Ulrich, R. Hafenbrak, P. Michler, L. Wang, A. Rastelli, and O. G. Schmidt, *Appl. Phys. Lett.* **91**, 051904 (2007).
- <sup>30</sup>M. Jaros, *Rep. Prog. Phys.* **48**, 1091 (1985).